LAWRENCE
LIVERMORE
NATIONAL
LABORATORY

LLNL-CONF-426106

Extended Simulations of Graphene Growth with Updated Rate Coefficients

R. Whitesides, X. You, M. Frenklach

March 19, 2010

Western States Section of the Combustion Institute Spring Meeting
Boulder, CO, United States
March 21, 2010 through March 23, 2010

Disclaimer

2010 Spring Technical Meeting
of the Western States Section of the Combustion Institute
Hosted by the University of Colorado at Boulder, Boulder, CO
March 21-23, 2010
Paper # 10S-50

Extended Simulations of Graphene Growth with Updated Rate Coefficients

Russell Whitesides[1], Xiaoqing You[2], and Michael Frenklach[2,3]

[1] *Lawrence Livermore National Laboratory, Livermore, CA 94550, USA*
[2] *Department of Mechanical Engineering, University of California, Berkeley, CA 94720-1740, USA*
[3] *Environmental Energy Technologies Division, Lawrence Berkeley National Laboratory, Berkeley, CA 94720, USA*

Abstract

New simulations of graphene growth in flame environments are presented. The simulations employ a kinetic Monte Carlo (KMC) algorithm coupled to molecular mechanics (MM) geometry optimization to track individual graphenic species as they evolve. Focus is given to incorporation of five-member rings and resulting curvature and edge defects. The model code has been re-written to be more computationally efficient enabling a larger set of simulations to be run, decreasing stochastic fluctuations in the averaged results. The model also includes updated rate coefficients for graphene edge reactions recently published in the literature. The new simulations are compared to results from the previous model as well as to hydrogen to carbon ratios recorded in experiment and calculated with alternate models.

1 Introduction

Soot production in practical combustion systems remains an unsolved problem leading to adverse effects on human health and the environment. Technical solutions to soot production require improved understanding of the underlying physics of its formation and destruction. The chemistry of these processes is one of the least-well understood aspects in this field. Recent modeling of soot chemistry has relied on the assumption of chemical similarity to polycyclic aromatic hydrocarbons (PAH) [1,2]. In this framework, kinetic Monte Carlo (KMC) simulations of PAH and graphene (essentially a PAH sheet) have been used to gain understanding into the dynamics of soot chemistry [3-14]. In these KMC simulations, the evolution of a PAH species or of a graphitic edge is tracked. In the predecessor to this work [5], a KMC model including detailed chemistry of a large number of surface reactions was presented. In this work, we present further

development of the model including significant code improvement, model updates, and application of the model to calculate C-H ratios with comparison to experimental data.

2 Model Development

The KMC simulation code has been completely re-written in a new language (Python versus MatLab) in a more efficient manner by reducing significantly the number of iteration loops and minimizing the stored data. The speedup of the code allows it to be run many more times at a given set of conditions. For example, in the previous version of the code the calculation of 15 stochastic simulations took approximately a week, while the same simulation can be run in about an hour in the updated coding.

The code was also altered to allow for simulation of varying environment. In previous simulations the environment was held constant to examine in detail the surface kinetics without the influence of changing temperature or gaseous species concentrations. The change makes it possible to simulate the evolution of an aromatic species in a simulated flame with temperature and species profiles calculated externally.

In addition to the code improvements, changes have been made to the included surface reactions. New reaction rates for six-member ring adsorption at an armchair site and at an embedded five-member ring site have been developed [3]. These updated rates have been included in the present simulations. In addition, because we are interested in comparing with benzene flame measurements, two new reactions are included allowing for adsorption and desorption of phenyl to an aromatic edge site. The rate coefficient for the phenyl adsorption is

$$1.98\times10^{76}T^{-18.90}\exp\left(-\frac{39470\ \text{cal/mol}}{RT}\right)$$

taken from [15]. This coefficient is a least squares fit of the modified Arhennius equation to the data from 500 to 2500 K from [16]. In the same work, Park et al. calculated the equilibrium constant for this reaction to be

$$1.45\times10^{-13}T^{3.23}\exp\left(3998\ \text{K}/T\right)$$

The resulting model was tested by re-computing previous results to ensure that the new coding produces similar results. In addition, the new simulations were run with an ensemble of 100 individual runs (each with a different starting random seed), thus reducing the stochastic fluctuations in the averaged data. The current model is also compared with results of the Raj et al. model [4] for C-H ratios measured in premixed flame experiments [17,18]. The species and temperature profiles were calculated using the Appel, Bockhorn, and Frenklach (ABF) kinetic mechanism [19] and the premixed flame model available in the Cantera code suite [20]. This is a similar method as used in [4] in order to create similar profiles. The ABF mechanism is composed of 101 species and 550 reactions. For flame A, an experimental temperature profile was reported by the experimenters and used in the simulations. In flame B the full energy equation was solved, as a temperature

profile was not available. The temperature profile and the concentration profiles for benzene, acetylene, hydrogen molecule and hydrogen atom were then used as inputs to the KMC simulations, which followed evolution of a pyrene molecule as it traveled through the flame. For the flame simulations, 1000 individual runs were performed with each run having a different starting random seed. The number of C and H atoms of the resulting species in each run were then checked at specified times corresponding to the burner heights of the measurements in the experiments. The relation of burner height to time was calculated by integration of the calculated velocity at each simulated grid point.

3 Results and Discussion

Comparison of simulations for the KMC model with previous coding and the updated coding were conducted starting with coronene as the starting species with environment held constant at 2000 K, pressure of 1 atm and gas phase composition $x_{C_2H_2}$ = x_{H_2} = 0.1, x_H = 0.01. This set of conditions was labeled the base case in [5]. For this comparison the rates of reactions are the same as they were in [5], i.e. they do not include the phenyl adsorption/desorption reactions and the updated rates presented in [3] (and discussed above) are not included. In Fig. 1, the growth rate and five-member ring fraction (f_{R5}) (both defined in [5]) are shown for the old and improved coding. For the old simulations, results are for an ensemble of 15 runs. In the new simulations results are shown for ensembles of both 15 and 100 runs. Agreement between the results of old and new simulations is good and shows that the re-written code has not affected the results. In addition the new simulations with a 100 run ensemble are less noisy, showing the decrease in stochastic fluctuations with increasing ensemble size.

Flame simulations were performed for two low-pressure premixed flames, which were experimentally examined by Homann and co-workers [17,18]. Flame A [18] (flame 2 in [4]) is fueled by benzene and flame B [17] (flame 4 in [4]) by acetylene. The conditions for these flames are given in Table 1. Figure 2 shows the calculated temperature and species concentrations for the two flames.

The C-H diagram for species produced in flame A is shown in Fig. 3. Four sets of data are plotted: the experimental measurement, the results reported by Raj et al. [4], and results from the present simulations with inclusion of phenyl adsorption/desorption (labeled PW1), and results from present simulations without phenyl adsorption/desorption (labeled PW2). Clearly, without phenyl adsorption/desorption our model significantly underpredicts growth of species in this flame as no species are seen having more than 34 carbon atoms while the experiment measured species up to 70 carbon atoms. This was expected as the fuel is benzene and direct adsorption should play a large role in the growth process. With the inclusion of the phenyl reactions, our model predicts more high carbon species, but still does not have as many as measured in experiment. The Raj et al. model has better agreement. One explanation can be found in that the Raj et al. model does not include the reverse reaction for phenyl adsorption. Leaving this reaction out of our model does produce larger species in our simulations. However,

we cannot physically justify exclusion of this reaction. Further explanation of this discrepancy will be sought in future work.

The C-H diagram for species produced in flame B is given in Fig. 4. The same four sets of data are shown for this flame as for flame A. In this case, the inclusion of phenyl adsorption/desorption reactions has very little effect on the resulting C-H ratios. Agreement between the experiment and both models is fairly good for this measurement.

In general, our present model tends to predict species with lower hydrogen content than the experiments. Five-member ring incorporation (included in our model but not in the Raj et al. model) leads to curved structures that have smaller edges relative to un-curved species with the same number of carbon (cf. Fig. 4 in [5]) and thus have fewer hydrogen atoms per molecule. In contrast, the model of Raj et al. tends to produce species with higher hydrogen content than those measured. This can be partially explained by lack of curvature and also in part by the large regions of "unavailable" sites produced when growing edges form finger like growth structures (cf. Fig. 15 in [4]). Inclusion of surface "rounding" reactions in a more recent publication [21] has improved this to some degree but does not achieve full agreement. The disagreement between the experiment and the models for C-H ratios may be a result of overprediction of curvature in our model and underprediction in the Raj et al. model. As discussed in our previous work [5], interlayer effects may hinder curvature and thereby reduce the rate of curvature inducing reactions.

4 Summary

We presented results from new development of a previously presented KMC model for PAH/graphene evolution. The new model incorporates code improvements, which greatly improved its speed, as well as new and updated rates for graphene edge reactions. The updated simulations were shown to produce similar results to the previous simulations with much shorter computational time. The new simulations were also compared with C-H ratios from experiment and from an alternate model. Both models and experiment are in agreement for a low-pressure, premixed, acetylene flame, however agreement is not as good for a similar flame fueled by benzene. The differences are likely due to differences in rate coefficients in the models as well as the inclusion of curvature inducing reactions in our current model. These discrepancies present avenues for further analysis of the surface processes included in the models.

Acknowledgements

R.W. was funded by DOE, Office of Vehicle Technologies, Gurpreet Singh and Kevin Stork, Technology Development Managers. This work performed under the auspices of the U.S. Department of Energy by Lawrence Livermore National Laboratory under Contract DE-AC52-07NA27344.

M.F. was supported by the Director, Office of Energy Research, Office of Basic Energy Sciences, Chemical Sciences, Geosciences and Biosciences Division of the US

Department of Energy, under Contract No. DE-AC03-76F00098. X.Y. and M.F. were supported by the US Army Corps of Engineers, Humphreys Engineering Center Support Activity, under Contract No. W912HQ-07-C-0044.

References

[1] M. Frenklach, H. Wang, Proc. Combust. Inst. 23 (1991) 1559-1566.
[2] M. Frenklach, Phys. Chem. Chem. Phys. 4 (2002) 2028-2037.
[3] X. You, R. Whitesides, D. Zubarev, W.A.J. Lester, M. Frenklach, Proc. Combust. Inst., submitted (2010).
[4] A. Raj, M. Celnik, R. Shirley, M. Sander, R. Patterson, R. West, M. Kraft, Combust. Flame 156 (2009) 896-913.
[5] R. Whitesides, M. Frenklach, J. Phys. Chem. A 114 (2010) 689-703.
[6] M. Frenklach, Proc. Combust. Inst. 26 (1996) 2285-2293.
[7] M. Frenklach, C.A. Schuetz, J. Ping, Proc. Combust. Inst. 30 (2005) 1389-1396.
[8] M. Celnik, A. Raj, R. West, R. Patterson, M. Kraft, Proc. Combust. Inst. 155 (2008) 161-180.
[9] M.S. Celnik, M. Sander, A. Raj, R.H. West, M. Kraft, Proc. Combust. Inst. 32 (2009) 639-646.
[10] A. Violi, A. Kubota, T. Truong, W. Pitz, C. Westbrook, A. Sarofim, Proc. Combust. Inst. 29 (2002) 2343-2349.
[11] A. Violi, Combust. Flame 139 (2004) 279-287.
[12] A. Violi, G.A. Voth, A.F. Sarofim, Proc. Combust. Inst. 30 (2005) 1343-1351.
[13] A. Violi, A. Venkatnathan, J. Chem. Phys. 125 (2006) 054302-8.
[14] S.H. Chung, A. Violi, Carbon 45 (2007) 2400-2410.
[15] H. Richter, S. Granata, W.H. Green, J.B. Howard, Proc. Combust. Inst. 30 (2005) 1397-1405.
[16] J. Park, S. Burova, A.S. Rodgers, M.C. Lin, J. Phys. Chem. A 103 (1999) 9036-9041.
[17] P. Weilmünster, A. Keller, K. Homann, Combust. Flame 116 (1999) 62-83.
[18] A. Keller, R. Kovacs, K. Homann, Phys. Chem. Chem. Phys. 2 (2000) 1667-1675.
[19] J. Appel, H. Bockhorn, M. Frenklach, Combust. Flame 121 (2000) 122-136.
[20] Cantera, <http://code.google.com/p/cantera/>.
[21] A. Raj, P.L. Man, T.S. Totton, M. Sander, R.A. Shirley, M. Kraft, Carbon 48 (2010) 319-332.

Tables

Table 1. Experimental conditions for modeled flames.

Flame	Pressure (kPa)	Fuel	x_{fuel}	x_{O_2}	Cold gas velocity (cm/s)	[C]/[O]	Ref.
A	2.67	C_6H_6	20.1	78.9	42	0.8	[18]
B	2.66	C_2H_2	50	50	42	1.0	[17]

Figures

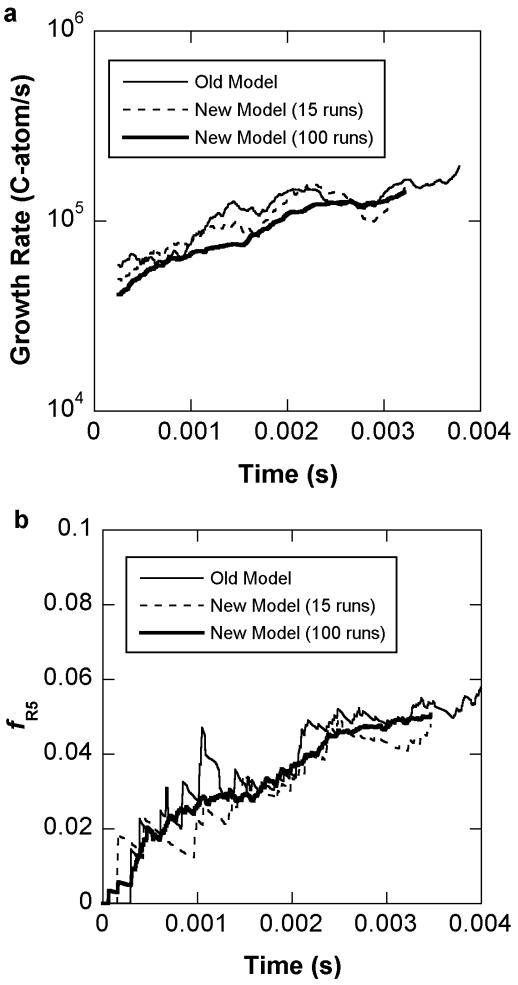

Fig. 1. Comparison of old and new model for (a) growth rate and (b) five-member ring fraction (f_{R5}).

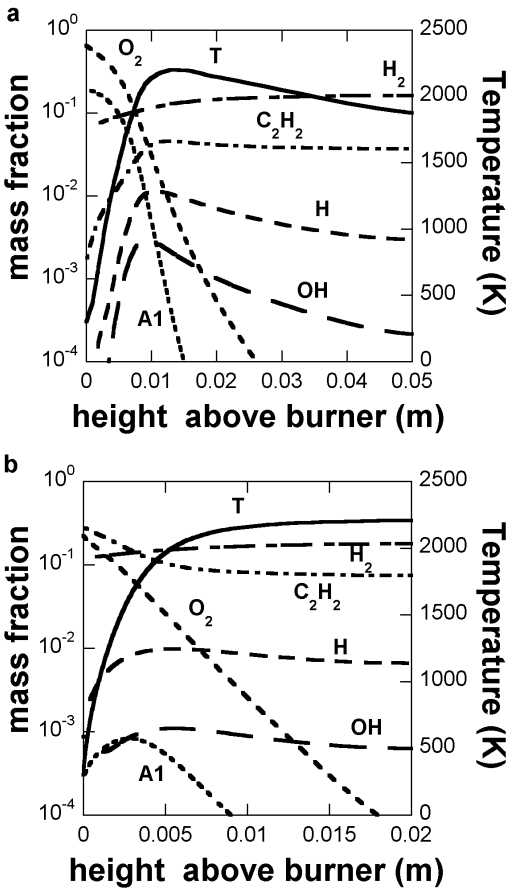

Fig. 2. Calculated temperature and concentration profiles for (a) flame A and (b) flame B.

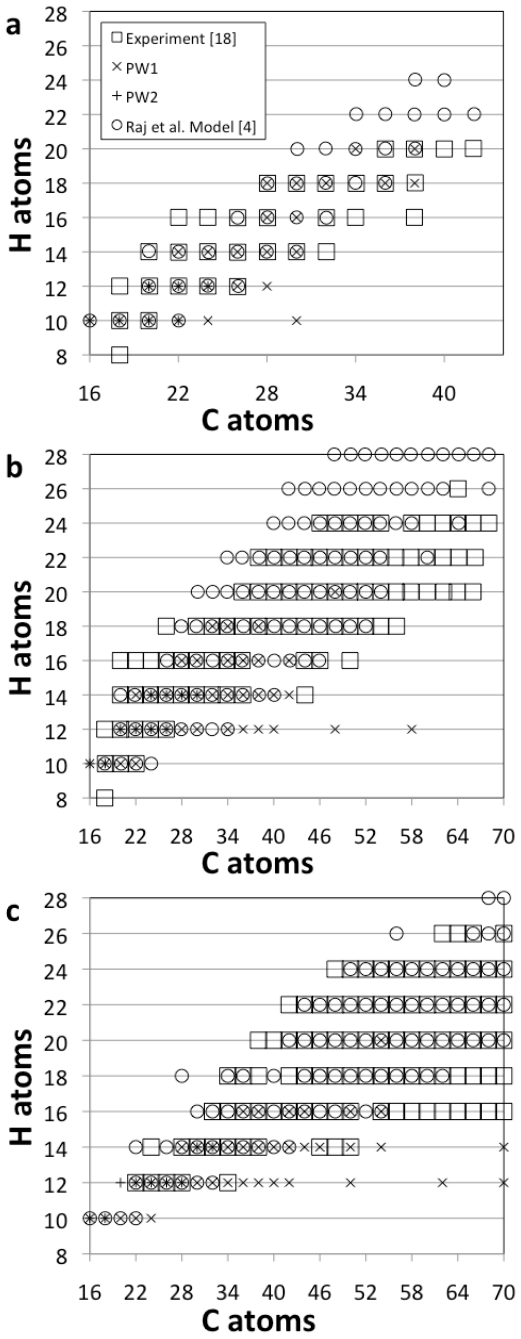

Fig. 3. C-H diagram for flame A for height above burner equal to (a) 5, (b) 7, and (c) 10 mm.

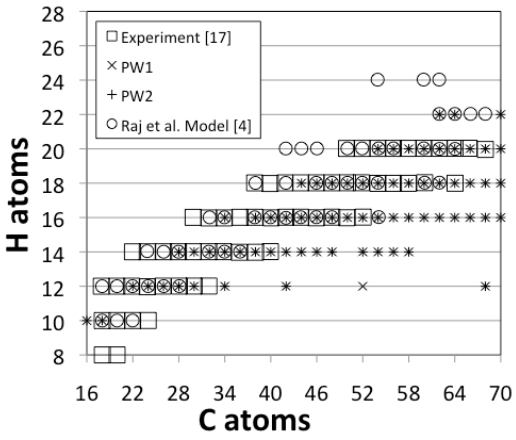

Fig. 4. C-H diagram for flame B at height above burner equal to 7 mm.